Article:
Zhao, Y., Armes, S.P. and An, Z. (2026) Mechanically robust ultrahigh molecular weight supramolecular hydrogels reinforced by synergistic chain entanglement, hydrogen bonding, and nanoparticle incorporation. Angewandte Chemie International Edition, 65 (24). e5675930. ISSN: 1433-7851

https://doi.org/10.1002/anie.5675930

Mechanically Robust Ultrahigh Molecular Weight Supramolecular Hydrogels Reinforced by Synergistic Chain Entanglement, Hydrogen Bonding, and Nanoparticle Incorporation

Yue Zhao[a], Steven P. Armes[c], and Zesheng An*[a,b]

[a] Y. Zhao, Prof. Z. An
State Key Laboratory of Supramolecular Structure and Materials
College of Chemistry, Jilin University
Changchun 130012 (China)
E-mail: anzesheng@jlu.edu.cn

[b] Prof. Z. An
Key Laboratory for Molecular Enzymology and Engineering of Ministry of Education
School of Life Sciences, Jilin University
Changchun 130012 (China)

[c] Prof. S. P. Armes
School of Mathematical and Physical Sciences
University of Sheffield
Sheffield, South Yorkshire, S3 7HF, UK

Supporting information for this article is given via a link at the end of the document.

Abstract: Tuning the mechanical properties of ultrahigh molecular weight (UHMW) physically crosslinked hydrogels remains a significant challenge. We address this by utilizing Fenton-initiated reversible addition-fragmentation chain transfer (RAFT) polymerization to synthesize poly(methacrylic acid) (PMAA) with molecular weights of up to 1,700 kg mol^{-1} under mild aqueous conditions. These UHMW polymers leverage extensive chain entanglement and hydrogen bonding to form strong and tough supramolecular hydrogels, exhibiting a tensile strength of up to 0.16 MPa, a fracture strain of 2000%, and a toughness of 2.93 MJ m^{-3}. Furthermore, the incorporation of PMAA-stabilized nanoparticles (spheres or worms) as secondary physical crosslinks significantly enhances energy dissipation and overall mechanical properties, resulting in a 2.5-fold increase in toughness relative to the neat UHMW PMAA hydrogel. This approach offers a versatile framework for designing high-performance soft materials through hierarchical molecular and nanoscale engineering.

Introduction

Poly(methacrylic acid) (PMAA) is an important water-soluble polymer that is widely used in drug delivery, biosensors, hydrogels, surface brushes, and water treatment owing to its excellent hydrophilicity, pH-responsiveness, and biocompatibility.[1] Traditionally, PMAA is synthesized via free-radical polymerization (FRP),[2] which provides rather limited control over molecular weight and architecture, thereby restricting the material's ultimate performance. More recently, reversible deactivation radical polymerization (RDRP) techniques have been employed to synthesize well-defined, low-dispersity PMAA.[3] Despite these synthetic advances, existing strategies are largely restricted to low molecular weights (typically M_n < 100 kg mol^{-1}). Moreover, such methods frequently require demanding conditions, such as elevated temperatures, strongly acidic media, high metal catalyst loadings, or organic solvents, which limit their practicality and sustainability. As a result, the controlled synthesis of high molecular weight PMAA under mild conditions remains a formidable challenge in polymer science.

Accessing ultrahigh molecular weight (UHMW, M_n > 1000 kg mol^{-1}) polymers via RDRP offers exciting prospects for investigating polymer physics on exceptionally large length scales and designing next-generation advanced functional materials.[4] The influence of chain entanglements is particularly evident for UHMW hydrogels. For example, Harrisson and Destarac demonstrated that UHMW triblock copolymers enable thermally induced gelation at remarkably low concentrations,[5] while Kopeć et al. revealed a transition in mechanical behavior from crosslinker-mediated elasticity to entanglement-dominated toughness in the UHMW regime.[6] We previously reported that increasing molecular weight significantly enhances the storage modulus for chemically crosslinked networks.[7] However, these systems typically yield either soft physical hydrogels or static, covalently crosslinked networks. The design of strong supramolecular hydrogels that combine extensive chain entanglement with reversible noncovalent bonding is highly desirable and may offer remarkable mechanical properties. We hypothesized that UHMW polymers that are capable of forming cooperative, reversible networks should bridge this gap. More specifically, UHMW PMAA represents a promising candidate, whereby extensive chain entanglements could be synergistically reinforced by strong hydrogen bonding via carboxylic acid dimer formation.[8]

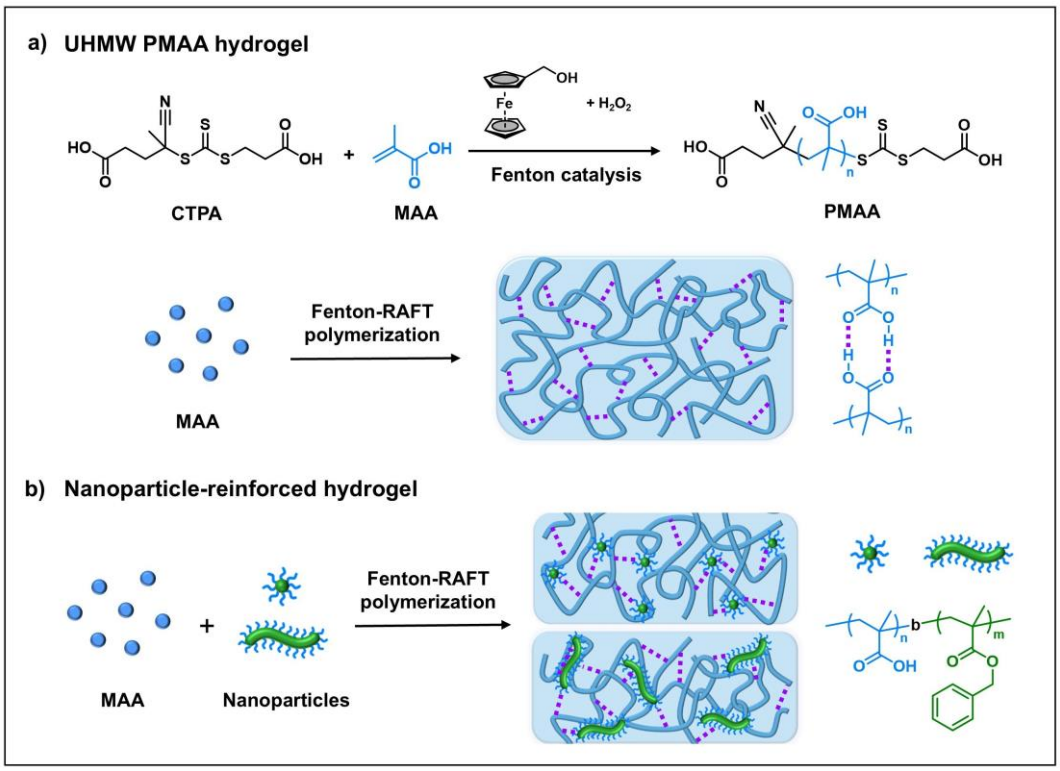

Scheme 1. a) Schematic representation of (a) Fenton catalyst-mediated RAFT polymerization of MAA for *in situ* hydrogel formation, and (b) fabrication of nanoparticle-reinforced PMAA hydrogels.

Herein, we address this challenge by developing ferrocenemethanol-mediated Fenton catalysis that enables the reversible addition-fragmentation chain transfer (RAFT)[9] polymerization of MAA directly in water at ambient temperature (**Scheme 1a**). This approach generates a sustained low flux of hydroxyl radicals, which is crucial for achieving controlled chain growth and suppressing termination, thereby yielding low-dispersity UHMW PMAA (M_n up to 1700 kg mol^{-1}). Remarkably, MAA polymerization directly results in the *in situ* formation of highly elastic, tough hydrogels, driven by the synergistic interplay of extensive chain entanglement and dynamic hydrogen bonding. Incorporating functional nanofillers has emerged as a powerful strategy to enhance mechanical properties.[10] Given that interfacial compatibility, stress transfer, and reinforcement efficiency are profoundly influenced by the nanofiller morphology,[10f] we incorporated well-defined PMAA-stabilized diblock copolymer spheres or worms into the PMAA network to create nanoparticle-loaded hydrogels that are reinforced by synergistic chain entanglement and hydrogen bonding (**Scheme 1b**). In contrast to previous work that employed nanoparticles as covalent crosslinkers,[11] we utilize hydrogen bond-mediated crosslinking to produce supramolecular hydrogels. This study not only resolves a longstanding challenge in the controlled synthesis of UHMW PMAA but also establishes a versatile framework for engineering high-performance soft materials that are both tough and strong.

Results and Discussion

Fenton-Initiated RAFT Polymerization

We and others have demonstrated that enzymatic catalysis can sustain a low radical flux during RDRP,[12] thus enabling the well-controlled synthesis of various UHMW polymers.[13] Inspired by these prior studies, we sought a catalytic system capable of operating under the inherent acidicity of a concentrated aqueous solution of MAA (30% w/v, pH ~ 2.5). Fenton catalysis was identified as an ideal candidate owing to its efficient production of hydroxyl radicals under such conditions and its proven efficacy as an initiator for RAFT polymerization.[12c, 13f, 14] After screening various catalysts, ferrocenemethanol (Fc-OH) coupled with H_2O_2 was selected for its favorable radical production profile and superior polymerization control (**Figures S1-S2**). RAFT polymerization of MAA was conducted directly in water at 30 °C using 4-((((2-carboxyethyl)thio)carbonothioyl)thio)-4-cyano-pentanoic acid (CTPA) as the RAFT agent. CTPA was chosen for its high water solubility and established efficacy for the controlled polymerization of methacrylic monomers.[15] Kinetic studies (**Figure 1a**) targeting a degree of polymerization (DP) of 1500 revealed pseudo-first-order behavior with near-quantitative conversion achieved within 10 h.

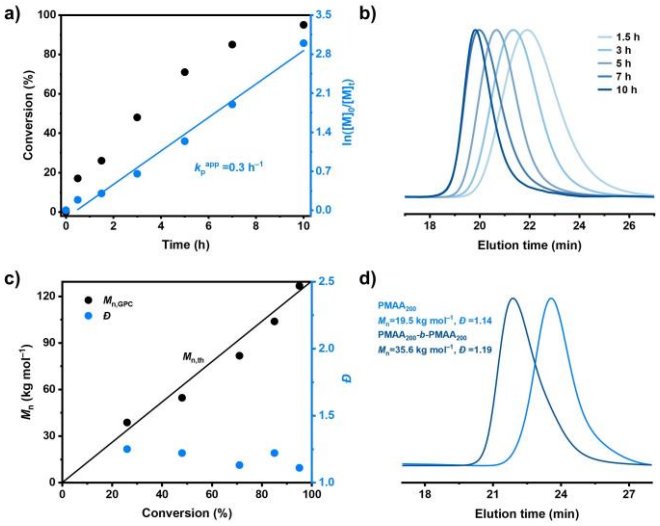

Figure 1. Kinetic data obtained for the Fenton-initiated RAFT homopolymerization of MAA using CTPA when targeting a DP of 1500: (a) MAA conversion and pseudo-first-order plot of ln([MAA]$_0$/[MAA]$_t$) versus time, (b) GPC traces recorded for the corresponding methylated polymers (PMMAs) obtained at varying time, and (c) plots of number-average molecular weight, M_n, and dispersity versus conversion. Conditions: [CTPA]/[Fc-OH]/[H_2O_2] = 1/0.05/0.1, 30 °C, [MAA]$_0$ = 30% w/v. (d) GPC traces recorded for a methylated PMAA$_{200}$ homopolymer and the corresponding chain-extended methylated PMAA$_{200}$-*b*-PMAA$_{200}$ pseudoblock copolymer.

Gel permeation chromatography (GPC) analysis of the corresponding methylated polymers revealed monomodal molecular weight distributions with experimental M_n data in good agreement with theoretical values and low dispersities ($Đ$ = 1.10). These results confirm the high degree of control afforded by this Fenton-RAFT system. Moreover, chain extension experiments (**Figure 1d)** indicated excellent end-group fidelity, as evidenced by complete reinitiation and a clear shift to higher molecular weight while maintaining a narrow molecular weight distribution.

Encouraged by these very promising results, we prepared a series of PMAA homopolymers with target DPs ranging from 500 to 30 000 (**Table 1**). High MAA conversions (> 90%) were consistently achieved without compromising control over the molecular weight distribution. For DPs ≤ 10 000, the number-average molecular weight, M_n, closely matched the theoretically predicted value and low dispersities were obtained ($Đ$ ≤ 1.20). For higher target DPs, slight deviations from theoretical values and higher dispersities were observed owing to inefficient chain transfer within the increasingly viscous reaction solution. Nevertheless, well-defined PMAA with M_n up to 1700 kg mol^{-1} ($Đ$ = 1.39) was obtained under optimized conditions. Furthermore, the versatility of this approach was demonstrated via statistical copolymerization of MAA with either *N*,*N*-dimethylacrylamide (DMA) or diacetone acrylamide (DAAM), yielding UHMW copolymers with similarly high efficiency.

Table 1. Summary of PMAA homopolymers and statistical copolymers synthesized via Fenton catalyst-mediated RAFT polymerization.

Entry[a]	F_{MAA}[b]	[M]/[CTPA]/[Fc-OH]/[H_2O_2]	Fc-OH (μM)	H_2O_2 (mM)	Time (h)	Conv.[c] (%)	$M_{n,th}$[d] (kg mol^{-1})	$M_{n,GPC}$[e] (kg mol^{-1})	$Đ$[e]
1		500/1/0.05/0.45	348	2.07	8	81	35	33	1.13
2		2000/1/0.05/1.5	87.0	1.16	11	91	157	158	1.17
3		5000/1/0.12/6	83.5	4.12	16	95	409	413	1.20
4	100%	10000/1/0.15/15	52.2	5.22	20	92	792	739	1.18
5		15000/1/0.3/20	69.6	4.64	24	95	1230	967	1.43
6		30000/1/0.35/35	40.6	4.06	24	85	2220	1650	1.39
7		15000/0/0.3/20	69.6	4.64	24	94	\	812	1.74
8[f]	90%	15000/1/0.3/20	68.4	2.85	20	99/99	1310	951	1.48
9[f]	80%	15000/1/0.3/20	67.5	2.81	20	99/99	1320	1190	1.28
10[f]	70%	15000/1/0.3/20	66.6	2.78	20	99/99	1340	980	1.37
11[g]	90%	15000/1/0.3/20	65.7	2.65	20	95/92	1500	1020	1.48

[a] Polymerization conditions: [MAA]$_0$ = 30% w/v, 30 °C. [b] MAA mole fraction. [c] Monomer conversion determined by ^{1}H NMR spectroscopy in either D_2O or DMSO-d_6. [d] Theoretical molecular weight: $M_{n,th} = M_{CTPA}$ + target DP × conv.% × M_{MAA}. [e] Experimental molecular weight and dispersity determined by GPC after methylation. [f] P(MAA-*co*-DMA). [g] P(MAA-*co*-DAAM).

Rheological and Compressive Performance

The ability to access a broad molecular weight range allows for precise tuning of hydrogel mechanical properties. Rheological characterization revealed that all PMAA hydrogels exhibited frequency-independent storage moduli (G′) that consistently exceeded the corresponding loss moduli (G″), characteristic of elastic-dominated, solid-like behavior (**Figure 2a and Figure S7**). Increasing M_n from 143 to 1400 kg mol^{-1} resulted in a two-fold enhancement in G′ (up to 70 kPa) (**Figure 2b**). This is attributed to the higher density of physical crosslinks derived from extensive chain entanglements. The PMAA hydrogels (pH ~ 2.5) underwent complete dissolution in deionized water (pH 6.8). Because this pH is above the pK_a (~ 5.0) of the methacrylic acid units, the deprotonation of carboxylic acid groups disrupts the sacrificial hydrogen bonds. The complete dissolution of the material, rather than mere swelling, confirms the absence of covalent crosslinks and highlights the supramolecular nature of the PMAA network.[17] In contrast, PMAA hydrogels prepared by conventional FRP exhibited poor reproducibility, as evidenced by the substantial discrepancy in modulus (15.5 kPa and 53.2 kPa) for samples prepared under identical conditions—a consequence of uncontrolled molecular weights. Furthermore, the maximum moduli attainable via FRP generally remain lower than those of UHMW PMAA hydrogels produced by Fenton-RAFT, primarily due to the inherent inability of FRP to reach comparable molecular weights. Notably, at equivalent molecular weights, the mechanical properties of both systems appear to be similar, despite the challenges of achieving such control with FRP. This suggests that molecular weight is the primary determinant of the mechanical properties in these supramolecular networks.

Initial mechanical assessments were performed via compression testing to evaluate the structural robustness of the PMAA hydrogels (Figure S8). As M_n increased from 158 to 1450 kg mol^{-1}, both the compressive strength and toughness increased substantially (by six-fold and seven-fold, respectively). The optimized UHMW PMAA hydrogels achieved a remarkable compressive strength of 64.2 MPa and a toughness of 2.4 MJ m^{-3}, maintaining macroscopic integrity even at 94% strain. This superior performance is attributed to the synergy between the dense chain entanglement network and the formation of carboxylic acid dimers, which facilitate efficient energy dissipation while preserving the structural integrity under high-load conditions. However, to more rigorously probe the fracture resistance and molecular dynamics of the system, we focused our subsequent analysis on the tensile properties and cyclic loading behavior.

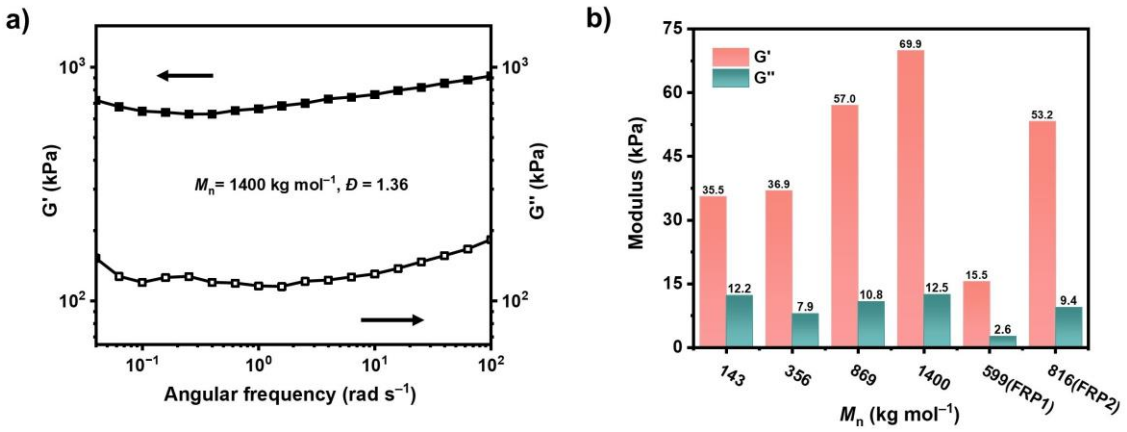

Figure 2. Rheological studies of PMAA hydrogels of varying molecular weights: (a) oscillatory rheological sweeps for UHMW PMAA hydrogels conducted at a constant strain of 1.0%, (b) variation of G' and G'' values with polymer molecular weight.

Tensile Properties

To more comprehensively evaluate the mechanical properties, we conducted systematical characterization on the hydrogels via tensile tests. The tensile tests (**Figure 3a)** revealed an initial elastic region followed by a pronounced plastic deformation regime beyond the yield point. The initial elasticity is attributed to chain uncoiling and bond stretching,[19] while the extended yield plateau indicates progressive chain disentanglement and the dynamic shuffling of hydrogen bonds.[20] As summarized in **Figure 3b**, both fracture strain (ε_b) and fracture stress (σ_b) increased monotonically with molecular weight. Although the σ_b values (up to 170 kPa) are moderate when compared to other hydrogel systems,[21] the exceptional ε_b (2000%) results in a remarkable toughness (up to 2.93 MJ m^{-3}). This value exceeds that of most reported physical hydrogels[22] and is comparable to that of certain sophisticated double-network systems.[23] The elastic modulus determined from the low-strain region (< 20%) of the stress–strain curve was 285 kPa, which is comparable to that reported for chemically crosslinked polyacrylamide hydrogels (357 kPa).[24] Importantly, such UHMW hydrogels exhibit superior tensile strength when compared to the corresponding FRP-derived PMAA hydrogels, which highlights the critical role of molecular weight and structural homogeneity in achieving high mechanical performance. FTIR analysis (**Figure S12**) revealed a broad O–H stretching vibration at ~3350 cm^{-1}, which is significantly red-shifted from the free O–H region (~3400–3500 cm^{-1}).[25] This indicates the formation of strong hydrogen bonding between the polymer chains and the aqueous medium. Furthermore, the C=O stretching vibration is located at 1645 cm^{-1}; this marked redshift relative to that of free C=O (~ 1730 cm^{-1})[26] confirms the participation of carbonyl groups in the formation of carboxylic acid dimers. Collectively, these spectroscopic features provide

evidence for the formation of hydrogen-bond-induced physical crosslinking.

Further tailoring was achieved via statistical copolymerization of MAA with either DMA or DAAM. These comonomers introduce additional hydrogen bonding sites or hydrophobic interactions (in the case of DAAM).[27] Copolymerization significantly increased the moduli and fracture stress, albeit with a reduction in fracture strain (**Figure 3d**). For example, UHMW P(DAAM-*co*-MAA) exhibited a 3.5-fold increase in fracture stress (0.56 MPa) and a 24-fold increase in elastic modulus (6.6 MPa) compared to that observed for the PMAA homopolymer (**Table S6**); such values are comparable to those reported for chemically cross-linked P(DMA-*co*-MAA) hydrogels.[28]

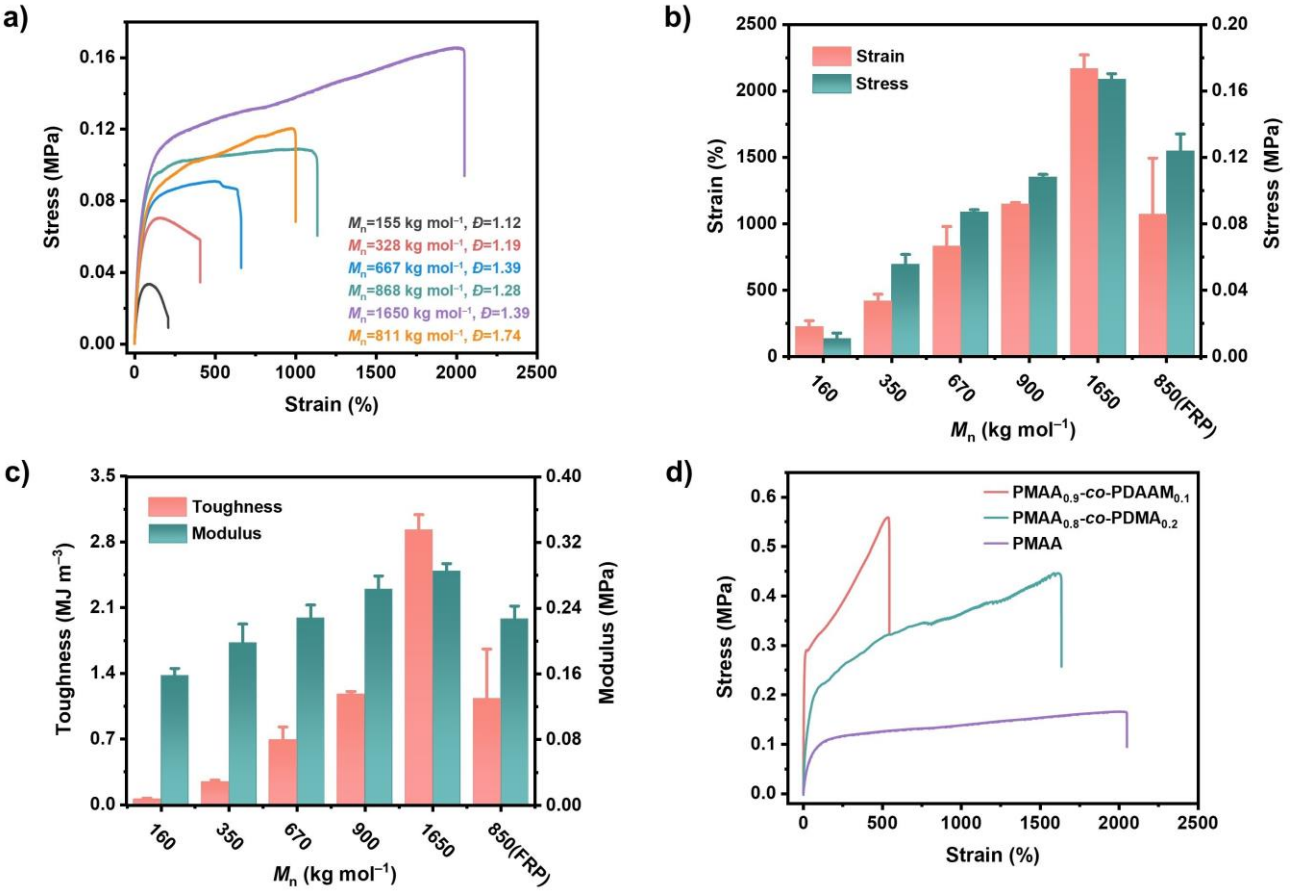

Figure 3. Tensile tests conducted on PMAA hydrogels of varying molecular weights: (a) tensile stress–strain curves of PMAA (cylindrical specimen: D = 4 mm, H = 10 mm ± 3 mm) at a constant strain rate of 0.1 s^{-1}, (b) summary of stress and strain at break, (c) summary of Young's modulus and toughness, (d) tensile stress–strain curves obtained for PMAA homopolymer and two statistical copolymers (DP = 15 000).

Nanoparticle-Reinforced Hydrogels

We hypothesized that these supramolecular PMAA hydrogels based on reversible hydrogen bonding and UHMW chain entanglements could be further reinforced by incorporating PMAA-stabilized diblock copolymer nanoparticles. Such nanoparticles can be conveniently prepared using polymerization-induced self-assembly (PISA),[29] a highly versatile and scalable method for synthesizing bespoke nano-objects with tailored surface chemistry and morphology. Specifically, dispersion polymerization of benzyl methacrylate (BzMA) using a PMAA$_{77}$ macromolecular chain transfer agent (macro-CTA) in ethanol produced well-defined PMAA$_{77}$-*b*-PBzMA$_{50}$ spheres (diameter = 24.4 nm, **Figure S16c**) and highly anisotropic PMAA$_{77}$-*b*-PBzMA$_{100}$ worms (cross-sectional diameter = 25.5 nm; sphere-equivalent diameter = 398 nm, **Figure S16f**).[30] Nanoparticle-reinforced PMAA hydrogels were subsequently fabricated by Fenton-catalyzed RAFT polymerization of MAA (target DP = 30 000) in the presence of varying amounts of such nanoparticles (**Scheme 1b**).

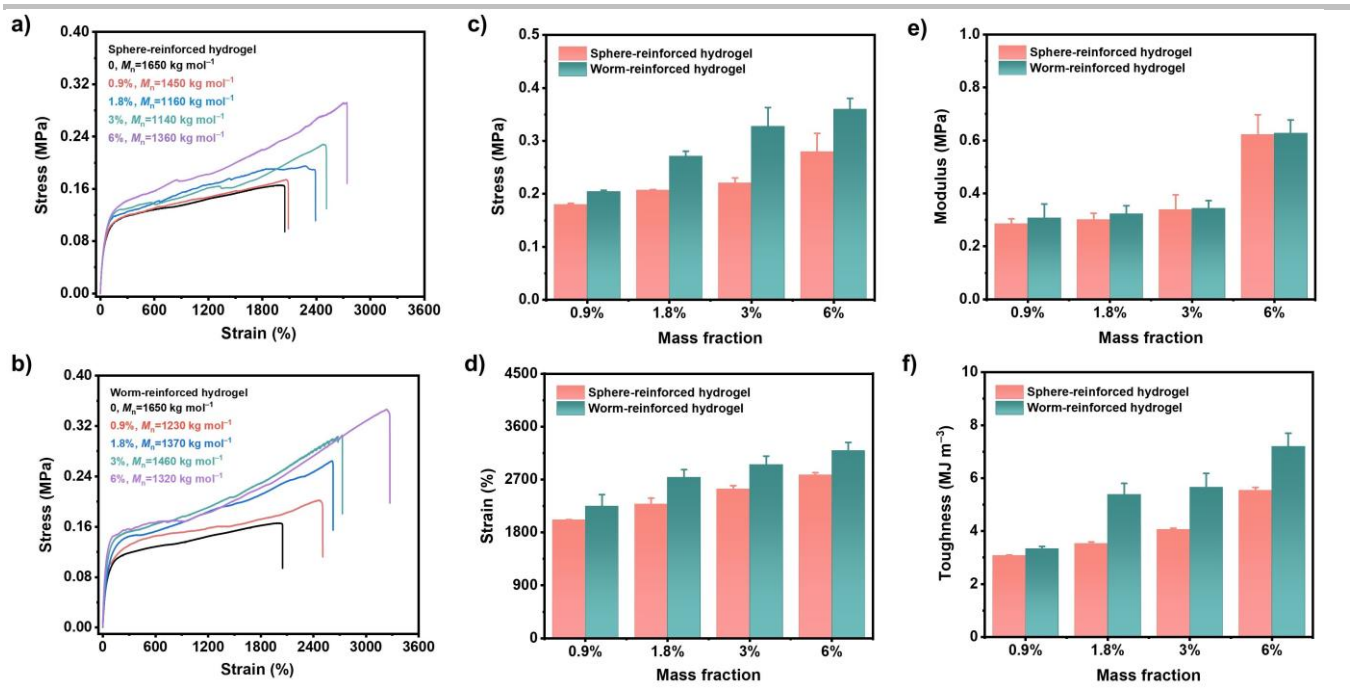

Figure 4. Tensile stress–strain curves for $PMAA_{30000}$ hydrogels reinforced by nanoparticles at various loadings: (a) sphere-reinforced PMAA hydrogels and (b) worm-reinforced PMAA hydrogels (cylindrical specimen, D = 4 mm, H = 10 mm ± 3 mm, measured at a constant strain rate of 0.1 s^{-1}). Comparison of tensile properties of nanoparticle-reinforced hydrogels at various nanoparticle loadings: (c) fracture stress, (d) fracture strain, (e) Young's modulus and (f) toughness.

Tensile analysis revealed that increasing the nanoparticle loading from 0.9% to 6% consistently enhanced the fracture stress, strain, and toughness (**Figure 4**). Notably, worm-like nanoparticles provided a more pronounced improvement compared to their spherical counterparts. This morphology-dependent reinforcement is attributed to the high aspect ratio and significant interfacial area, which allows them to effectively bridge and facilitate extensive hydrogen bonding with the UHMW polymer chains. These anisotropic worms act as efficient nanoscale sacrificial units and topological obstacles that hinder chain slippage. Their presence facilitates long-range stress transfer and provides an additional energy dissipation pathway through the reversible "bridge-and-slip" of chians along the nanoparticle surface, effectively preventing localized failure.[11b, 31]

To elucidate the molecular mechanism underlying the observed mechanical properties, we performed stepwise cyclic tensile loading–unloading tests on selected UHMW PMAA hydrogels by progressively increasing the strain amplitude (**Figure S11**). This method is a standard protocol for probing the internal network dynamics of hydrogels.[32] The loading curves exhibit significant hysteresis loops, which we attribute to the reversible rupture of hydrogen-bonded carboxylic acid dimers acting as sacrificial units. While initial loading curves closely followed a single master curve, the unloading curves exhibited increasing residual strain with higher strain amplitudes. This suggests that the ultrahigh extensibility is governed by the **synergy between the dense entanglement network**, which prevents macroscopic failiure, and the **dynamic hydrogen bonding**, which facilitates efficient energy dissipation.[33] To further investigate the energy dissipation mechanisms, both the neat UHMW PMAA hydrogel and the worm-reinforced hydrogels were subjected to fifty consecutive loading–unloading cycles at 150% strain without inter-cycle rest intervals (**Figure 5**). The first cycle revealed a large hysteresis loop and significant residual strain, which is consistent with substantial energy dissipation via the irreversible rupture of a subset of sacrificial hydrogen bonds and chain reorganization (**Figure 5a,b**).[34] In subsequent cycles, the hysteresis area decreased markedly and stabilized, indicating that while the first cycle disrupted the initial as-prepared state, the remaining physical crosslinks are highly reversible and capable of rapid reformation.[35] We propose that these UHMW hydrogels constitute a **dual-scale hierarchical network**: the carboxylic acid hydrogen-bonded dimers serve as **fast-exchange dynamic units** that enable continuous energy dissipation, while the UHMW chain entanglements function as a **slow-relaxing structural backbone**, ensuring macroscopic integrity and conferring excellent fatigue resistance.

Notably, the stabilized hysteresis ratio of the worm-reinforced hydrogel was approximately double that of the neat UHMW PMAA hydrogel (**Figure 5c**), clearly demonstrating that the incorporation of worm-like nanoparticles enhances energy dissipation within the PMAA network.[11b, 11c] This improvement is attributed to the relatively large interfacial area and highly anisotropic nature of the worm-like nanoparticles, which promotes the efficient reorganization of dynamic hydrogen bonds and act as nanoscale sacrificial units. This efficient energy dissipation mechanism is ultimately responsible for the enhanced fracture energy and toughness of the composite hydrogel.

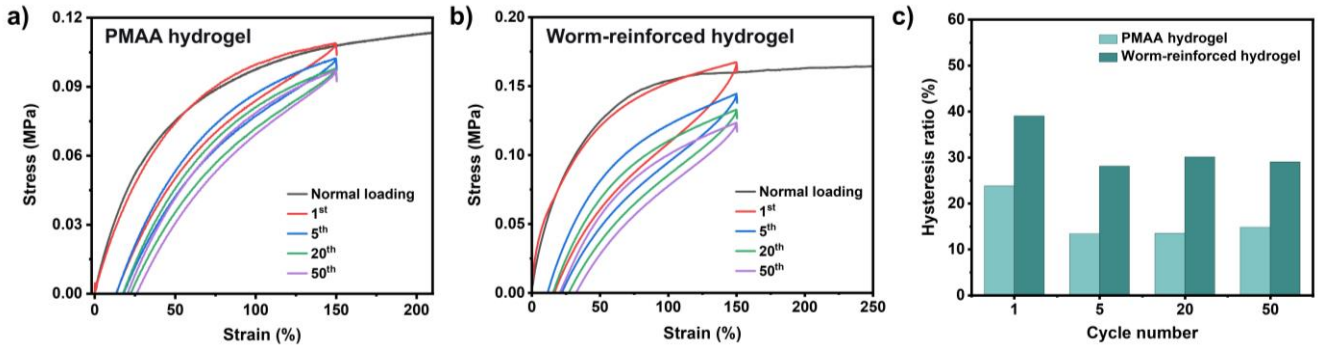

Figure 5. Tensile stress–strain cycling at a strain = 150%: (a) PMAA hydrogel, (b) worm-reinforced hydrogel, and (c) comparison of hysteresis ratios.

Conclusion

We have developed a Fenton catalyst-initiated RAFT polymerization protocol that provides remarkable control over the synthesis of PMAA under mild aqueous conditions, enabling convenient access to molecular weights up to 1700 kg mol^{-1}. This method allows for the *in situ* formation of supramolecular PMAA hydrogels that exhibit excellent mechanical properties, owing to the synergistic effect of extensive chain entanglement and dense hydrogen bonding. Integrating PMAA-stabilized nanoparticles—particularly highly anisotropic diblock copolymer worms—further enhanced the energy dissipation for such supramolecular networks, resulting in simultaneous improvements in modulus, strength, strain, and toughness. This work highlights the critical importance of ultrahigh molecular weight in the design of high-performance soft materials and provides a versatile strategy for engineering tough, strong supramolecular hydrogels for future load-bearing applications.

Supporting Information

Experimental details, additional NMR spectra, UV-vis spectra, fluorescence spectra, GPC traces, stress–strain curves of compression and tensile, FTIR spectra and polymerization data can be found in the Supporting Information.

Acknowledgements

We thank the National Key Research and Development Program of China (2021YFA1501600) and the National Natural Science Foundation of China (22193020, 22193024, 22371089) for financial support.

Keywords: RAFT • poly(methacrylic acid) • Fenton catalysis • ultrahigh molecular weight • nanoparticle

[1] a) K. Y. Lee, D. J. Mooney, *Chemical Reviews* **2001**, *101*, 1869-1880; b) M. Morishita, T. Goto, K. Takayama, N. A. Peppas, *Journal of Drug Delivery Science and Technology* **2006**, *16*, 19-24; c) B. Städler, A. D. Price, A. N. Zelikin, *Advanced Functional Materials* **2011**, *21*, 14-28; d) K. Gong, L. Hou, P. Wu, *Advanced Materials* **2022**, *34*, 2201065; e) Y. Shi, B. Wu, S. Sun, P. Wu, *Nature Communications* **2023**, *14*, 1370; f) W. Zhao, B. Wu, Z. Lei, P. Wu, *Angewandte Chemie International Edition* **2024**, *63*, e202400531; g) Z. Qu, H. Xu, H. Gu, *ACS Applied Materials & Interfaces* **2015**, *7*, 14537-14551.

[2] M. Buback, R. A. Hutchinson, I. Lacík, *Progress in Polymer Science* **2023**, *138*, 101645.

[3] a) L. Couvreur, C. Lefay, J. Belleney, B. Charleux, O. Guerret, S. Magnet, *Macromolecules* **2003**, *36*, 8260-8267; b) E. J. Ashford, V. Naldi, R. O'Dell, N. C. Billingham, S. P. Armes, *Chemical Communications* **1999**, 1285-1286; c) C. Burguière, S. Pascual, C. Bui, J.-P. Vairon, B. Charleux, K. A. Davis, K. Matyjaszewski, I. Bétremieux, *Macromolecules* **2001**, *34*, 4439-4450; d) M. Fantin, A. A. Isse, A. Venzo, A. Gennaro, K. Matyjaszewski, *Journal of the American Chemical Society* **2016**, *138*, 7216-7219; e) L. Fu, A. Simakova, M. Fantin, Y. Wang, K. Matyjaszewski, *ACS Macro Letters* **2018**, *7*, 26-30; f) K. Matyjaszewski, *Macromolecules* **2012**, *45*, 4015-4039; g) I. Chaduc, M. Lansalot, F. D'Agosto, B. Charleux, *Macromolecules* **2012**, *45*, 1241-1247.

[4] a) Z. An, *ACS Macro Letters* **2020**, *9*, 350-357; b) S. Zhu, W. Kong, S. Lian, A. Shen, S. P. Armes, Z. An, *Nature Synthesis* **2025**, *4*, 15-30; c) S. Lian, R. Li, Y. Chen, Z. An, *Macromolecules* **2025**, *58*, 5385-5394; d) R. Li, S. P. Armes, Z. An, *Angewandte Chemie-International Edition* **2025**; e) R. Li, S. Zhang, X. Tang, G. G. Qiao, S. P. Armes, Z. An, *Journal of the American Chemical Society* **2025**, *147*, 33153-33161; f) X. Tang, L.-Q. Meng, R. Li, S. Zhu, S. Lian, B. Jia, Z. An, *Angewandte Chemie-International Edition* **2025**.

[5] L. Despax, J. Fitremann, M. Destarac, S. Harrisson, *Polymer Chemistry* **2016**, *7*, 3375-3377.

[6] G. Irvine, K. Myronidis, F. Pinto, M. Kopeć, *Angewandte Chemie International Edition* **2025**, *64*, e202421970.

[7] W. Kong, Z. An, *CCS Chemistry* **2025**, *8*, 1467-1479.

[8] E. Raphael, M. J. Derry, M. Hippler, S. P. Armes, *Chemical Science* **2021**, *12*, 12082-12091.

[9] J. Chiefari, Y. K. Chong, F. Ercole, J. Krstina, J. Jeffery, T. P. T. Le, R. T. A. Mayadunne, G. F. Meijs, C. L. Moad, G. Moad, E. Rizzardo, S. H. Thang, *Macromolecules* **1998**, *31*, 5559-5562.

[10] a) Z. Zhao, R. Fang, Q. Rong, M. Liu, *Advanced Materials* **2017**, *29*, 1703045; b) P. Lavrador, M. R. Esteves, V. M. Gaspar, J. F. Mano, *Advanced Functional Materials* **2021**, *31*, 2005941; c) C.-H. Lu, Y.-C. Yeh, *Small* **2021**, *17*, 2105997; d) K. Haraguchi, T. Takehisa, *Advanced Materials* **2002**, *14*, 1120-1124; e) M. Mehrali, A. Thakur, C. P. Pennisi, S. Talebian, A. Arpanaei, M. Nikkhah, A. Dolatshahi-Pirouz, *Advanced Materials* **2017**, *29*, 1603612; f) T. Ienn, C. Lo Van, R. Brunel, D. Albertini, E. Chamczyk, P. Alcouffe, G. Sudre, F. Lortie, J. Bernard, *Angewandte Chemie International Edition* **2026**, *65*, e18861.

[11] a) Z. Zhao, M. Huo, *Polymer Chemistry* **2024**, *15*, 1577-1590; b) L. Fan, Z. Zeng, R. Zhu, A. Liu, H. Che, M. Huo, *Chemistry of Materials* **2022**, *34*, 6408-6419; c) Z. Zhao, L. Fan, G. Song, M. Huo, *Chemistry of Materials* **2024**, *36*, 1436-1448; d) Y. Du, S. Jia, Y. Chen, L. Zhang, J. Tan, *ACS Macro Letters* **2021**, *10*, 297-306.

[12] a) R. Li, W. Kong, Z. An, *Macromolecules* **2023**, *56*, 751-761; b) R. Li, W. Kong, Z. An, *Angewandte Chemie International Edition* **2022**, *61*, e202202033; c) A. Reyhani, M. D. Nothling,

H. Ranji-Burachaloo, T. G. McKenzie, Q. Fu, S. Tan, G. Bryant, G. G. Qiao, *Angewandte Chemie International Edition* **2018**, *57*, 10288-10292.
[13] a) Z. Liu, Y. Lv, Z. An, *Angewandte Chemie International Edition* **2017**, *56*, 13852-13856; b) F. Zhou, R. Li, X. Wang, S. Du, Z. An, *Angewandte Chemie International Edition* **2019**, *58*, 9479-9484; c) R. Li, Z. An, *Angewandte Chemie International Edition* **2020**, *59*, 22258-22264; d) R. Li, S. Zhang, Q. Li, G. G. Qiao, Z. An, *Angewandte Chemie International Edition* **2022**, *61*, e202213396; e) R. Li, S. Zhang, X. Tang, G. G. Qiao, S. P. Armes, Z. An, *Journal of the American Chemical Society* **2025**; f) A. Reyhani, S. Allison-Logan, H. Ranji-Burachaloo, T. G. McKenzie, G. Bryant, G. G. Qiao, *Journal of Polymer Science Part A: Polymer Chemistry* **2019**, *57*, 1922-1930.
[14] a) A. Reyhani, T. G. McKenzie, H. Ranji-Burachaloo, Q. Fu, G. G. Qiao, *Chemistry – A European Journal* **2017**, *23*, 7221-7226; b) Y. Zhao, S. Zhang, Z. An, *Angewandte Chemie International Edition* **2025**, *64*, e202421851.
[15] a) G. Moad, E. Rizzardo, S. H. Thang, *Accounts of Chemical Research* **2008**, *41*, 1133-1142; b) S. Perrier, *Macromolecules* **2017**, *50*, 7433-7447; c) M. R. Hill, R. N. Carmean, B. S. Sumerlin, *Macromolecules* **2015**, *48*, 5459-5469; d) M. D. Nothling, Q. Fu, A. Reyhani, S. Allison-Logan, K. Jung, J. Zhu, M. Kamigaito, C. Boyer, G. G. Qiao, *Advanced Science* **2020**, *7*, 2001656.
[16] a) I. Dellatolas, T. Divoux, E. Del Gado, I. Bischofberger, *Soft Matter* **2026**, *22*, 2290-2300; b) D. Durand, M. Delsanti, M. Adam, J. M. Luck, *Europhysics Letters* **1987**, *3*, 297.
[17] a) V. Kozlovskaya, E. Kharlampieva, M. L. Mansfield, S. A. Sukhishvili, *Chemistry of Materials* **2006**, *18*, 328-336; b) E. Kharlampieva, I. Erel-Unal, S. A. Sukhishvili, *Langmuir* **2007**, *23*, 175-181.
[18] a) S. V. Wanasinghe, M. Sun, K. Yehl, J. Cuthbert, K. Matyjaszewski, D. Konkolewicz, *ACS Macro Letters* **2022**, *11*, 1156-1161; b) C. W. A. Bainbridge, A. Wangsadijaya, N. Broderick, J. Jin, *Polymer Chemistry* **2022**, *13*, 1484-1494.
[19] T. L. Sun, T. Kurokawa, S. Kuroda, A. B. Ihsan, T. Akasaki, K. Sato, M. A. Haque, T. Nakajima, J. P. Gong, *Nature Materials* **2013**, *12*, 932-937.
[20] R. Xue, X. Xin, L. Wang, J. Shen, F. Ji, W. Li, C. Jia, G. Xu, *Physical Chemistry Chemical Physics* **2015**, *17*, 5431-5440.
[21] S. Lin, X. Liu, J. Liu, H. Yuk, H.-C. Loh, G. A. Parada, C. Settens, J. Song, A. Masic, G. H. McKinley, X. Zhao, *Science Advances*, *5*, eaau8528.
[22] M. E. Seitz, D. Martina, T. Baumberger, V. R. Krishnan, C.-Y. Hui, K. R. Shull, *Soft Matter* **2009**, *5*, 447-456.
[23] a) K. Yasuda, J. Ping Gong, Y. Katsuyama, A. Nakayama, Y. Tanabe, E. Kondo, M. Ueno, Y. Osada, *Biomaterials* **2005**, *26*, 4468-4475; b) Q. M. Yu, Y. Tanaka, H. Furukawa, T. Kurokawa, J. P. Gong, *Macromolecules* **2009**, *42*, 3852-3855; c) T. Nakajima, H. Sato, Y. Zhao, S. Kawahara, T. Kurokawa, K. Sugahara, J. P. Gong, *Advanced Functional Materials* **2012**, *22*, 4426-4432.
[24] S. Tan, C. Wang, B. Yang, J. Luo, Y. Wu, *Advanced Materials* **2022**, *34*, 2206904.
[25] J.-J. Max, C. Chapados, *The Journal of Chemical Physics* **2010**, *133*, 164509.
[26] M. Tammer, *Colloid and Polymer Science* **2004**, *283*, 235-235.
[27] Y. Yilmaz, *Journal of Chemical Physics* **2007**, *126*, 224501.
[28] X. Hu, M. Vatankhah-Varnoosfaderani, J. Zhou, Q. Li, S. S. Sheiko, *Advanced Materials* **2015**, *27*, 6899-6905.
[29] a) S. L. Canning, G. N. Smith, S. P. Armes, *Macromolecules* **2016**, *49*, 1985-2001; b) N. J. W. Penfold, J. Yeow, C. Boyer, S. P. Armes, *ACS Macro Letters* **2019**, *8*, 1029-1054; c) F. D'Agosto, J. Rieger, M. Lansalot, *Angewandte Chemie International Edition* **2020**, *59*, 8368-8392; d) C. Liu, C. Y. Hong, C. Y. Pan, *Polymer Chemistry* **2020**, *11*, 3673-3689; e) E. J. Cornel, J. H. Jiang, S. Chen, J. Z. Du, *CCS Chemistry* **2021**, *3*, 2104-2125; f) C. György, S. P. Armes, *Angewandte Chemie-International Edition* **2023**, *62*, e202308372; g) S. Zhang, R. Li, Z. An, *Angewandte Chemie-International Edition* **2024**, *63*, e202315849.
[30] a) M. Semsarilar, E. R. Jones, A. Blanazs, S. P. Armes, *Advanced Materials* **2012**, *24*, 3378-3382; b) C. Gonzato, M. Semsarilar, E. R. Jones, F. Li, G. J. P. Krooshof, P. Wyman, O. O. Mykhaylyk, R. Tuinier, S. P. Armes, *Journal of the American Chemical Society* **2014**, *136*, 11100-11106; c) M. Semsarilar, V. Ladmiral, A. Blanazs, S. P. Armes, *Polymer Chemistry* **2014**, *5*, 3466-3475.
[31] a) Y. S. Thio, J. Wu, F. S. Bates, *Macromolecules* **2006**, *39*, 7187-7189; b) J. M. Dean, N. E. Verghese, H. Q. Pham, F. S. Bates, *Macromolecules* **2003**, *36*, 9267-9270; c) T. Ienn, C. Lo Van, R. Brunel, D. Albertini, E. Chamczyk, P. Alcouffe, G. Sudre, F. Lortie, J. Bernard, *Angewandte Chemie International Edition* **2025**, *n/a*, e18861; d) W. F. M. Daniel, J. Burdyńska, M. Vatankhah-Varnoosfaderani, K. Matyjaszewski, J. Paturej, M. Rubinstein, A. V. Dobrynin, S. S. Sheiko, *Nature Materials* **2016**, *15*, 183-189; e) Z. Heng, X. Zhang, Y. Chen, H. Zou, M. Liang, *Chemical Engineering Journal* **2019**, *360*, 542-552.
[32] a) J. P. Gong, *Soft Matter* **2010**, *6*, 2583-2590; b) R. E. Webber, C. Creton, H. R. Brown, J. P. Gong, *Macromolecules* **2007**, *40*, 2919-2927; c) G. Gao, G. Du, Y. Sun, J. Fu, *ACS Applied Materials & Interfaces* **2015**, *7*, 5029-5037.
[33] a) C. E. R. Edwards, D. J. Mai, S. Tang, B. D. Olsen, *Physical Review Materials* **2020**, *4*, 015602; b) R. Zhu, D. Zhu, Z. Zheng, X. Wang, *Nature Communications* **2024**, *15*, 1344; c) F. Puza, Y. Zheng, L. Han, L. Xue, J. Cui, *Polymer Chemistry* **2020**, *11*, 2339-2345; d) J. Kim, G. Zhang, M. Shi, Z. Suo, *Science* **2021**, *374*, 212-216.
[34] M. Hua, S. Wu, Y. Ma, Y. Zhao, Z. Chen, I. Frenkel, J. Strzalka, H. Zhou, X. Zhu, X. He, *Nature* **2021**, *590*, 594-599.
[35] X. Li, K. Cui, Y. Zheng, Y. N. Ye, C. Yu, W. Yang, T. Nakajima, J. P. Gong, *Science Advances*, *9*, eadj6856.

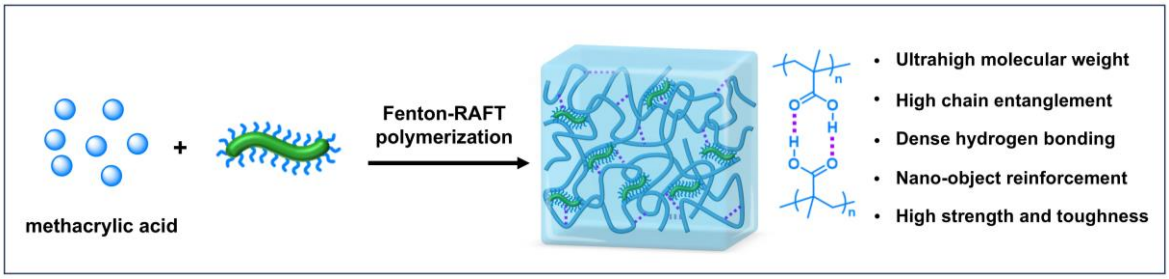

Fenton-initiated RAFT polymerization enables the controlled synthesis of ultrahigh molecular weight poly(methacrylic acid) (PMAA) under mild aqueous conditions. The resulting chains form supramolecular hydrogels *in situ* with high elasticity, strength, and toughness. Furthermore, incorporating PMAA-stabilized worm-like nanoparticles significantly enhances the energy dissipation capacity. This work highlights the critical importance of ultrahigh molecular weight in the design of high-performance soft materials through hierarchical molecular and nanoscale engineering.